Sequential Learning of the Pareto Front for Multi-objective Bandits

Elise Crépon, Aurélien Garivier, Wouter M Koolen

Sequential Learning of the Pareto Front for Multi-objective Bandits

élise crepon[1]
ENS Lyon

Aurélien Garivier
ENS Lyon

Wouter M. Koolen
CWI and Twente University

Abstract

We study the problem of sequential learning of the Pareto front in multi-objective multi-armed bandits. An agent is faced with K possible arms to pull. At each turn she picks one, and receives a vector-valued reward. When she thinks she has enough information to identify the Pareto front of the different arm means, she stops the game and gives an answer. We are interested in designing algorithms such that the answer given is correct with probability at least $1 - \delta$. Our main contribution is an efficient implementation of an algorithm achieving the optimal sample complexity when the risk δ is small. With K arms in d dimensions p of which are in the Pareto set, the algorithm runs in time $O(Kp^d)$ per round.

1 INTRODUCTION

Stochastic multi-armed bandits have emerged as a fundamental framework for studying sequential learning. In the classic setting of scalar rewards, the UCB algorithm solves the regret minimization problem and the Track-and-Stop algorithm solves the best arm identification problem. In this paper we are interested in the extension to vector-valued rewards, which is the arena for multi-criterion optimization. Here the problem of identifying the best arm generalizes to identifying the subset of arms with Pareto optimal means [Auer et al., 2016]. We study this problem in the fixed confidence setting. That is, the learner is given a confidence parameter. She sequentially collects noisy vector-valued rewards from a finite-armed bandit. After having collected enough data, the learner stops and outputs a subset of arms. The goal of the learner is to identify with high probability the correct Pareto set. Our approach is based on instantiating the Track-and-Stop framework [Garivier and Kaufmann, 2016] to the Pareto front identification problem so as to obtain an algorithm with optimal sample complexity [2]. The Track-and-Stop framework has recently seen tremendous success across pure exploration problems in bandits and RL. Examples include best arm identification in Spectral [Kocák and Garivier, 2021], Stratified [Russac et al., 2021], Lipschitz [Degenne et al., 2019], Linear [Degenne et al., 2020, Jedra and Proutiere, 2020], Dueling [Haddenhorst et al., 2021], Contextual [Tirinzoni et al., 2020, Hao et al., 2020] and Markov bandits [Moulos, 2019]. Other objectives include Top-m identification [Chen et al., 2017b, Chen et al., 2017a], MaxGap identification [Katariya et al., 2019], Thresholding [Garivier et al., 2017], Monte Carlo Tree Search [Garivier et al., 2016], optimal policy identification in MDPs [Al Marjani and Proutiere, 2021], and minimizing Tail-Risk [Agrawal et al., 2021]. The framework has also been instantiated to Pareto front identification [Kone et al., 2023]. The Track-and-Stop template is in some sense universal: the starting point is an information-theoretic, instance-dependent sample complexity lower bound of min-max form (see our Proposition 1 below). The learning algorithm is designed to match this lower bound by solving (an estimate of) that min-max problem. For that, in turn, it suffices to calculate a certain gradient [Degenne et al., 2019]. Yet here the details become problem-specific, in the sense that the tractability of this gradient computation varies across problems. Some identification objectives have closed-form solutions, some have efficient special-purpose optimizers, some can leverage a reduction to generic convex optimization, and for others nothing much is known. An overarching methodology remains elusive, and as such it is important to extend our toolbox by solving particular hard cases, of which Pareto front identification is a prime example. Our contribution is, at its core, an efficient imple-

Proceedings of the 27th International Conference on Artificial Intelligence and Statistics (AISTATS) 2024, Valencia, Spain. PMLR: Volume 238.

[1] preferred capitalization

[2] This can be either asymptotic optimality as in the original [Garivier and Kaufmann, 2016], or some later finite confidence refinement [Degenne et al., 2019].

mentation [3] of the gradient computation required for executing Track-and-Stop for Pareto front identification. With that problem-specific computational kernel implemented, the general scheme instantiates and we obtain an instance-optimal fixed confidence learner. Our combinatorial and algorithmic innovations reduce the run-time in p from the naive exponential $O(Kd^{p+1})$ to polynomial $O(Kp^d)$ per round. This is a reasonable computation cost for instances with a large number of arms and a small number of objectives.

We conclude here by mentioning extensions and alternative versions. [Kone et al., 2023] study approximate Pareto front identification. Skyline identification is a special case of Pareto front identification [Cheu et al., 2018]. Multi-objective optimization is also studied from a regret minimization perspective. Achieving a vector-valued expected reward not too far from the Pareto front (in some distance metric) is studied, both in stochastic and adversarial bandits [Busa-Fekete et al., 2017, Xu and Klabjan, 2023]. [Zuluaga et al., 2013] motivates the relevance of studying multi-ojective optimization.

1.1 Setting

We use the setting of multi-objective multi-armed bandits, which is the following: given K independent probability distributions on $\mathbb{R}^d$, $\nu = (\nu_k)_{k\in[K]} \in V$, with respective means $\mu = (\mu_k^j)_{k\in[K],j\in[d]}$, at every time step $t \in \mathbb{N}$ an agent gets to pick an arm $A_t \in [K]$ and receives an independent reward $X_t \in \mathbb{R}^d$ drawn from ν_{A_t}. The objective here is not to maximize cumulative reward over time but to identify as fast as possible (under a correctness constraint) the best performing arms. However, since we are in a multi-objective setting, we have no way of identifying a single best performing arm as we could do in a single objective framework: an arm might perform really well on one objective $j \in [d]$ but get poor results on another one, or an arm could rank averagely but on all the objectives. We have no way of discriminating one against the other.

For that reason, we are interested in identifying all the Pareto optimal arms. To be Pareto optimal, an arm must not be dominated by another one which means having its performance on all of the objectives be poorer than a single other arm. An arm which would have another one dominating it, is one about which we are sure that it has a better counter part, whereas an arm which as no one dominating it is optimal since we have no way of comparing how different objective compare with each other. We are then interested in identifying all of the Pareto optimal arms as fast as possible. Letting $\mathcal{F}_t = \sigma(X_1, \cdots, X_t)$ be the sigma-field generated by the observations up to time t. A strategy is then defined by *a sampling rule* $(A_t)_t$ where $A_t \in [K]$ is $\mathcal{F}_{t-1}$ measurable, *a stopping rule* τ, which is a stopping time with respect to $(\mathcal{F}_t)_t$, and *an answer rule* $P_\tau \subseteq [K]$ that is $\mathcal{F}_\tau$-measurable, which is the set of arm indices the learner assumes to be the Pareto set.

Given a risk $\delta > 0$, we call a strategy δ-PAC if it ensures that the answers it gives at the end of its runs are correct with a confidence δ, i.e. $\mathbb{P}(P_\tau \text{ is wrong}) \leq \delta$. This family of problem is called *pure exploration* and has already been well studied, in particular in the case where a single answer is correct which is our case. We apply the results from the literature to our specific problem. Also notice that while our setting is mainly focused on multi-objective, it includes the single-objective framework within the special case $d = 1$. This well-studied case of best-arm identification will serve as a reference throughout the paper, some of the difficulties that we present having their (degenerated) equivalent in dimension 1.

1.2 Pareto optimality

To formalize the definition of the Pareto set, we introduce the following binary relation. An arm with distribution ν on $\mathbb{R}^d$ and mean $\mu \in \mathbb{R}^d$ is said to be *dominated* by an arm ν' with mean μ', which we denote by $\nu \preceq \nu'$ (or equivalently $\mu \preceq \mu'$) iff $\forall j \in [d], \mu_j \leq \mu'_j$. This means that ν' performs better than ν on all the d different objectives. For a specific μ, we create a partial order between the indices of the arms given by $k_0 \preceq_\mu k_1 \iff \mu_{k_0} \preceq \mu_{k_1}$. This comparison is a partial order but is not connected, hence within a finite set it may have multiple maxima. We call these maxima the (strict) Pareto set and we denote it by $p(\mu) \triangleq \max_{\preceq_\mu}[K] = \arg\max_{\preceq, k\in[K]} \mu_k$. The Pareto set is defined as the indices of the points rather than the points directly because while our leaner has access to the indices, it doesn't have access to the points directly.

In this paper, we give an algorithm based on Track-and-Stop to identify the Pareto set of multi-variate Gaussians. We provide a careful analysis of its complexity. We also tackle the special case of dimension two and give an improved complexity in this case. In the first section of this paper, we give a formal definition of Pareto optimality. In Section 2, we recall the Track-and-Stop framework and motivate why it applies to our problem. In Section 3, we detail our algorithm and analyze its complexity.

[3] The source code used to run all experiments included in the paper is available at `https://github.com/elise-crepon/sequential-pareto-learning-experiments`.

2 LOWER BOUND ON THE SAMPLE COMPLEXITY AND ALGORITHM

This section uses the results of [Garivier and Kaufmann, 2016] to derive a lower bound on the sample complexity and to find an efficient algorithm to solve our problem.

We use the formalism of active sequential hypotheses learning. We let M be a set of K arms bandit models and $\mathcal{H} = \{\mathcal{H}_i \,|\, i \in [n]\}$ a finite set of disjoint hypotheses (which is a partition of M). We introduce $h : M \to \mathcal{H}$ which is the function that associates to any $\nu \in M$ the only $\mathcal{H}_i$ that contains ν. We are interested in algorithms that can identify the hypothesis that contains ν. The sampling, stopping and answer rules defined in the introduction still holds only the final answer given is H_τ the hypothesis the learner assumes the models they are interacting with is in. In this context, a δ-PAC strategy is any strategy that can ensure that $\mathbb{P}_\nu(\nu \in H_\tau)(= \mathbb{P}_\nu(h(\nu) = H_\tau)) \leq \delta$ for all $\nu \in M$.

We denote by $\mathrm{Alt}(\nu) \triangleq \{\nu' \in M \,|\, h(\nu') \neq h(\nu)\} = h(\nu)$ the subset of our model space M which contains all the models that have a different answer than the one of ν. This set of models is important because for a player to make a mistake they need to confuse the model they get samples from with a model in $\mathrm{Alt}(\nu)$. Hence for any algorithm to stop, it needs to get enough information to distinguish the current model from all models in $\mathrm{Alt}(\nu)$ with risk at most δ.

[Garivier and Kaufmann, 2016] introduce the following lower bound for the number of samples needed for active sequential hypotheses testing with a unique valid hypothesis in the bandit framework.

Proposition 1 (Sample complexity lower bound)**.** *Given a set of models M, a finite set of disjoint hypotheses $\mathcal{H} = (\mathcal{H}_i)_{i\in[n]}$ which is a partition of M and a risk parameter $\delta > 0$, any δ-PAC strategy is such that for every $\nu \in M$:*

$$\mathbb{E}_\nu(\tau_\delta) \geq \mathrm{kl}(\delta, 1-\delta) \cdot T^*(\nu) \;,$$

where

$$T^*(\nu)^{-1} \triangleq \sup_{w\in\triangle_K} \inf_{\lambda\in\mathrm{Alt}(\nu)} \sum_{k\in[K]} w_k \,\mathrm{KL}(\nu_k, \lambda_k) \;.$$

Our task of Pareto set identification is an instance of this problem: our hypotheses are for each subset of arms $[K]$ the set of models for which this set is the Pareto set. For a given model, the only correct hypothesis is the one associated with its Pareto set and the models in $\mathrm{Alt}(\nu)$ are such that their Pareto set is not the same as that of ν.

$$\mathrm{Alt}(\nu) \triangleq \{\nu' \in V \,|\, p(\nu') \neq p(\nu)\} \;. \tag{1}$$

As noted in the same paper, this lower bound hints us toward an efficient sampling rule. If we were to know ν, then the maximizer w^* of the optimization problem $T^*(\nu)$ gives us the fastest sampling rule that is able to make the difference between ν and the models in $\mathrm{Alt}(\nu)$. However, we don't know ν upfront. The Track-and-Stop algorithm proposes to solve the optimization problem with estimates of the model and to correct for possible bias with some forced exploration. The algorithm also comes with a stopping and recommendation rule that we import from the literature.

However, using this algorithm requires us to be able to solve the optimization problem behind $T^*(\nu)$. For best arm identification, [Garivier and Kaufmann, 2016] propose a clever yet special-purpose algorithm. However, that approach does not work for Pareto set identification making the problem much harder. Since, for

$$D_w(\nu, \lambda) \triangleq \sum_{k\in[K]} w_k \,\mathrm{KL}(\nu_k, \lambda_k) \;,$$

the function $w \in \triangle_K \mapsto \inf_{\lambda\in\mathrm{Alt}(\nu)} D_w(\nu, \lambda)$ is concave with respect to w, we can learn it using gradient ascent. Moreover, as we are refining our estimates at each time step, we can do an online gradient ascent and do only one step of the gradient ascent per time step. In order to perform gradient ascent, we need to be able to solve and find the minimizer of

$$\begin{array}{ll} \min & D_w(\nu, \lambda) \;. \\ \text{w.r.t.} & \lambda \in \mathrm{Alt}(\nu) \end{array} \tag{2}$$

However, the computation of the minimal transportation cost from ν to a $\lambda \in \mathrm{Alt}(\nu)$ that changes the Pareto set is not a convex function and requires a specific solving procedure. Because it carries more geometric intuition, we tackle here the case of Gaussian random variables with identity covariance (i.e. the objectives are independent from one another). Hence, our models are fully parametrized by their means μ, which we use as a stand-in for ν when talking about them. Our main contribution is to propose an efficient algorithm to solve this optimization problem in the case of Gaussian random variables. We provide a general analysis for higher dimensions and refine it for the case of dimension two. Under these assumptions, the w-weighted transportation cost D_w between two models equals:

$$D_w(\mu, \lambda) \triangleq \sum_{k\in[K]} \frac{w_k}{2} ||\mu_k - \lambda_k||^2 \;. \tag{3}$$

Though we will focus only on solving this specific optimization problem for the rest of the paper without delving in the inner workings of the Track-and-Stop

algorithm, we give here a few details on how we instantiate it. Once we obtain a gradient in w from solving (2) at a specific w, we do a single step of the Hedge algorithm using the gradient-norm-adaptive tuning. Both taking a single optimization step and this specific gradient ascent algorithm are detailed in the literature. See [Degenne et al., 2019, Degenne et al., 2020, Wang et al., 2021] for references.

3 MINIMIZING THE TRANSPORTATION COST

We give in this section a general procedure to compute the minimal transportation cost between μ and a λ that changes the Pareto front. We show that the computation of this cost can be split in two sub-procedures that are independent from each other. We analyze the complexity of each of these algorithms.

Theorem 1 (Algorithmic complexity of the minimal transportation cost)**.** *The minimal transportation cost* (2) *to change the Pareto front of our multi-variate Gaussians model* (3) *and its minimizer can be computed in*

$$O\left(\left(K(p+d)+d^3p\right)\binom{p+d-1}{d-1}\right),$$

where p is the number of Pareto optimal points in our model.

We introduce the following lemma, with proof in Appendix A, to help us find the solution to (2) by splitting Alt as defined in (1) in subpieces on which the optimization will be more easily done.

Lemma 1 (Splitting the domain)**.** *Let $\mu, \lambda \in \mathbb{R}^{Kd}$*

$$p(\mu) \neq p(\lambda) \iff \exists\{k_0,k_1\} \subseteq p(\mu) : k_0 \preceq_\lambda k_1 \\ \vee \exists k_0 \notin p(\mu) \forall k \in p(\mu) : k_0 \not\preceq_\lambda k\,.$$

In words, for λ to have a different Pareto set than μ it is necessary and sufficient that either a point from the Pareto set of μ is dominated in λ by another point from the Pareto set of μ, or that a point that is on the Pareto set of μ is no longer dominated in λ by any of the points from the Pareto set of μ. Splitting the problem this way allows us to design efficient procedures to find the minimum transportation cost from μ to a λ that changes its Pareto set.

Given $\mu \in \mathbb{R}^{Kd}$, we define

$$\mathrm{Alt}^{\mathrm{rm}} : \{k_0,k_1\} \subseteq p(\mu) \mapsto \{\lambda \in \mathbb{R}^{Kd} \,|\, k_0 \preceq_\lambda k_1\} \text{ and}$$
$$\mathrm{Alt}^{\mathrm{add}} : k_0 \notin p(\mu) \mapsto \{\lambda \in \mathbb{R}^{Kd}_, | \forall k \in p(\mu)\, k_0 \not\preceq_\lambda k\}\,.$$

Lemma 1 allows us to say that $\mathrm{Alt}^{\mathrm{add}}(k_0)$ for all $k_0 \notin p(\mu)$ and $\mathrm{Alt}^{\mathrm{rm}}(k_0,k_1)$ for all $\{k_0,k_1\} \subseteq p(\mu)$ provide a covering of $\mathrm{Alt}(\mu)$. We can thus solve the minimization independently for each of them and then take the minimal value of these as our minimal transportation cost:

$$\mathrm{Alt}(\mu) = \left(\bigcup_{\{k_0,k_1\}\subseteq p(\mu)} \mathrm{Alt}^{\mathrm{rm}}(k_0,k_1)\right) \\ \cup \left(\bigcup_{k_0\notin p(\mu)} \mathrm{Alt}^{\mathrm{add}}(k_0)\right). \tag{4}$$

We will now refer to the first case as removing a point from the Pareto set and to the second one as adding a point on the Pareto set, but we want to emphasize that the first case won't necessary yield the smallest cost to remove the given point from the Pareto set and the second one will not necessarily add the focused point to the Pareto set.

3.1 Removing a point from the Pareto set

In this section we prove the following lemma:

Lemma 2 (Cost of removing a point from the Pareto set)**.** *Given $\{k_0,k_1\} \subseteq p(\mu)$, the minimal transportation cost for*

$$\begin{array}{ll} \min & D_w(\mu,\lambda) \\ w.r.t. & \lambda \in \mathrm{Alt}^{\mathrm{rm}}(k_0,k_1) \end{array} \tag{5}$$

is

$$\frac{1}{2}\frac{w_{k_0}w_{k_1}}{w_{k_0}+w_{k_1}} \sum_{j\in[d]} \left(\max\{0,\mu^j_{k_0}-\mu^j_{k_1}\}\right)^2.$$

This cost and the associated minimizer can be computed in $O(d)$ and then the algorithmic complexity for all $\mathrm{Alt}^{\mathrm{rm}}$ is $O(p^2d)$.

Proof. Let $\{k_0,k_1\} \subseteq p(\mu)$, we are interested in computing the smallest transportation cost from μ to λ such that in λ the point k_1 now dominates k_0. Moving any other point than k_0 and k_1 in λ doesn't affect whether k_1 dominates k_0, hence this is superfluous and would only cost us more, so we can restrict our analysis to λ that only moves k_0 and k_1. Now, let $\mathcal{J}$ be the set of dimensions alongside which $\mu^j_{k_0} \geq \mu^j_{k_1}$. Since our transportation cost is separable alongside each dimension, then moving our points alongside any other axis that the ones in $\mathcal{J}$ would not help create the domination and would bear some extraneous cost. As such we can restrict ourselves to λ that only move k_0 and k_1 alongside $\mathcal{J}$. Using again that the transportation cost separability, we can split our analysis along the different axis independently. Now, the cost of inverting $\mu^j_{k_0}$ and $\mu^j_{k_1}$ for $j \in \mathcal{J}$ is a known problem from best arm identification. We compute the value here but it

is possible to see [Garivier and Kaufmann, 2016] for a reference. So our optimization problem boils down to

$$\inf_{x_\lambda \le y_\lambda} w_x \frac{1}{2}(x_\mu - x_\lambda)^2 + w_y \frac{1}{2}(y_\mu - y_\lambda)^2 \ .$$

The inf will be reached at a point where $x_\lambda = y_\lambda \triangleq s$. Taking the derivative in s of the cost function, we get $w_x(s - x_\mu) + w_y(s - y_\mu)$ which is null at $s^* \triangleq \frac{w_x x_\mu + w_y + y_\mu}{w_x + w_y}$ yielding the following minimum transportation cost $\frac{1}{2}\frac{w_x w_y}{w_x + w_y}(x_\mu - y_\mu)^2$. Now summing alongside the axis of $\mathcal{J}$ yields

$$\frac{1}{2}\frac{w_{k_0} w_{k_1}}{w_{k_0} + w_{k_1}} \sum_{j \in [d]} (\mu^j_{k_0} - \mu^j_{k_1})^2_+$$

where $(\cdot)^2_+ : u \mapsto (\max\{0, u\})^2$ stands for the squared positive part.

Computing the cost of shadowing a point by another and conversely is then done in $O(d)$ operations, which we need to do for each pair of points in the Pareto set leading us to a computation cost of $O(p^2 d)$ for removing a point. We highlight the difference between K and p as for large values of K, p might be significantly lower than K. □

We present in Appendix D a speed-up for the dimension two from time $O(p^2)$ to time $O(p)$, and we discuss why this speed-up is not possible in higher dimensions $d > 2$.

3.2 Adding a point to the Pareto set

The cost of adding a point to the Pareto set doesn't have a closed expression as was the case for removing a point. It is a more tedious procedure, which shows in the final algorithmic complexity.

Lemma 3 (Cost of adding a point to the Pareto set)**.** *Consider the minimum transportation cost to add any point to the Pareto set*

$$\begin{array}{ll} \min & D_w(\mu, \lambda) \ . \\ \textit{w.r.t.} & \lambda \in \bigcup_{k_0 \notin p(\mu)} \mathrm{Alt}^{\mathrm{add}}(k_0) \end{array} \tag{6}$$

The value and minimizer can be computed in time

$$O\left(\big(K(p+d) + d^3 p\big) \binom{p+d-1}{d-1} \right) .$$

To prove this lemma, we start by looking at how, given a target location λ_0 for a point $k_0 \notin p(\mu)$, points from the Pareto set should move to ensure that they are no longer dominating λ_0. We then provide an algorithm to range over all the different possible ways points from the Pareto set can move. Then, given a way the points from the Pareto set move, we compute the minimal transportation cost and the associated minimizer coherent with this way of moving points from the Pareto set.

Let $k_0 \notin p(\mu)$. We want to find a λ such that in λ, all points from $p(\mu)$ are no longer dominating k_0 as outlined before. For ease of notation, we use 0 as a stand-in for k_0 in our subscripts.

We study for now a weaker version of our problem, see Figure 1. Given a point λ_0 to which we will transport μ_0, what is the minimal cost to move the points from $p(\mu)$ to break their domination of k_0. This question is independent for all points in the Pareto set as they are not interacting with each others costs, so we can treat them one by one. For a given point k of the Pareto set, we are only interested in making one of its coordinates below the corresponding entry of λ_0. Now, either moving μ_0 to λ_0 already pushed μ_k outside of the upper orthant of k_0 or we need to get it outside of the way. In the first case, the transportation cost is zero, in the other one, as our transportation cost is separable alongside every dimension, we only need to find the dimension alongside which the transportation cost is the smallest i.e. $\frac{w_k}{2} \min_j (\mu^j_k - \lambda^j_0)^2$. We can put the two expressions together as $\frac{w_k}{2} \min_{j \in [d]} (\mu^j_k - \lambda^j_0)^2_+$ where $(\cdot)^2_+$ is the square of the positive part which is a convex, non-decreasing and differentiable function. Putting all of the points back together, we get that given λ_0, the minimal transportation cost to move everyone from $p(\mu)$ outside of its top right orthant is

$$g_{k_0}(\lambda_0) \triangleq \frac{w_0}{2} ||\mu_0 - \lambda_0||^2 + \sum_{k \in p(\mu)} \frac{w_k}{2} \min_{j \in [d]} (\mu^j_k - \lambda^j_0)^2_+ .$$

Finding the smallest transportation cost is then equivalent to finding the minimal value of g which we now set out to do. First, it is possible to move all of the $\min_j$ out to the start of the function giving us $g_{k_0}(\lambda_0) = \min_{\varphi : p(\mu) \to [d]} g_{k_0, \varphi}(\lambda_0)$ where $g_{k_0,\varphi}$ has the same expression as g_{k_0} but with $\min_j \mu^j_k - \lambda^j_0$ replaced by $\mu^{\varphi(k)}_k - \lambda^{\varphi(k)}_0$. Hence $\inf_{\lambda_0 \in \mathbb{R}^d} g_{k_0}(\lambda_0) = \min_\varphi \inf_{\lambda \in \mathbb{R}^d} g_{k_0,\varphi}(\lambda_0)$. The $g_{k_0,\varphi}$ are differentiable strictly convex functions, which makes them quite easy to minimize.

The idea is now to range over all different $\varphi : p(\mu) \to [d]$, to compute the minimizer of $g_{k_0,\varphi}$ and to take the minimum over all of those. However following this procedure would lead to a computation cost in $\Omega(d^p)$ which is exponential in the number of arms in the Pareto set and thus would for most use case represent to high of a computation cost to reasonably use the algorithm. Our main insight and the key to tractability is that it is not necessary to consider all elements in $[d]^{p(\mu)}$. Instead, it turns out that we need only look at a subset (which depends on the bandit μ) of size $O(p^{d-1})$

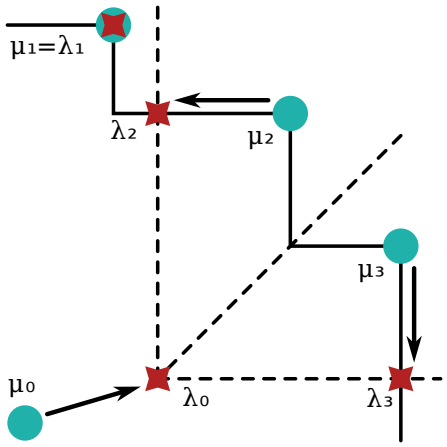

Figure 1: The original model is drawn in turquoise (circle). We start by moving the point 0 to a new location. Then we move the points that are still in its all-positive orthant outside of it with respect to the dimension where the move is the shortest (brown stars).

polynomial in the number of arms. To understand why, let λ_0 and let $\varphi : p(\mu) \to [d]$, the mapping from $k \in p(\mu)$ to $\arg\min_j \mu_k^j - \lambda_0^j$. The set $S(\varphi)$ of λ_0 that yield the same φ map is given by the following linear system

$$\forall k \in p(\mu), \forall j \in [d], \quad \mu_k^{\varphi(k)} - \lambda_0^{\varphi(k)} \leq \mu_k^j - \lambda_0^j \ .$$

For all $k_0 \notin p(\mu), \lambda_0 \in S(\varphi)$, we know that $\forall \varphi' : [p] \to [d]$, $g_{k_0,\varphi}(\lambda_0) \leq g_{k_0,\varphi'}(\lambda_0)$. Given a φ, $S(\varphi)$ is called the cell associated with φ. However, while for any point λ_0 there is a cell $S(\varphi)$ that contains it, the converse is not the case and a cell associated with a φ might well be empty. A cell is empty if

$$\forall \lambda_0, \exists \varphi' : g_{k_0,\varphi'}(\lambda_0) < g_{k_0,\varphi}(\lambda_0) \ .$$

A φ map associated with a non-empty cell is called valid. Ranging over the φ with an empty cell is useless, thus, we can restrict our $\min_\varphi$ to valid φ.

We highlight the fact that while $S(\varphi)$ is the subset of $\mathbb{R}^d$ is the set of points where $g_{k_0,\varphi}$ is lower than all other $g_{k_0,\varphi'}$, the minimizer in λ_0 of $g_{k_0,\varphi}$ might not leave with $S(\varphi)$. However, this is not a cue to consider the constrained problem where λ_0 is restricted to live in $S(\varphi)$ as studying the unconstrained problem would still yield the correct overall minimizer.

Also, note that $S(\varphi)$ doesn't depend on k_0 neither through μ_{k_0} or w_{k_0} but only on λ_0 as such a cell being empty or not doesn't depend on the point that we might be currently considering. Hence, we can start by enumerating all non-empty cells and then for each of them we compute the minimizer of $g_{k_0,\varphi}$ for every different $k_0 \in p(\mu)$, which avoids us enumerating K different times the non-empty cells. We thus introduce

$$g_\varphi = \min_{k_0 \notin p(\mu)} g_{k_0,\varphi} \text{ and } g = \min_{\varphi : S(\varphi) \neq \varnothing} g_\varphi$$

and we get that

$$\inf_{\lambda_0 \in \mathbb{R}^d} g(\lambda_0) = \min_{\varphi : S(\varphi) \neq \varnothing} \min_{k_0 \notin p(\mu)} \inf_{\lambda_0 \in \mathbb{R}^d} g_{k_0,\varphi}(\lambda_0) \ .$$

In the next section, we give an algorithm to find non-empty cells and we provide an analysis on the number of them and the algorithmic complexity of our algorithm to range over non-empty cells.

3.2.1 Constructing cells

Using the observations from the previous section, to know if a cell is empty or not, we could just range over all possible $\varphi : p(\mu) \to d$ and when one of them has a non-empty $S(\varphi)$ we compute the minimizer of g_φ. Let $U \subseteq V \subseteq p(\mu)$ and $\varphi^r : U \to [d]$ and $\varphi : V \to [d]$. First, we provide a new altered definition for $S(\varphi)$ which is still compatible with the first one, but which now works with maps with a restricted domain:

$$S(\varphi) = \left\{ \lambda_0 \in \mathbb{R}^d \middle| \begin{array}{r} \forall k \in \mathrm{dom}(\varphi), \forall j \in [d], \\ \mu_k^{\varphi(k)} - \lambda_0^{\varphi(k)} \leq \mu_k^j - \lambda_0^j \end{array} \right\}.$$

We know assume that $\varphi|_U = \varphi^r$, we have that $S(\varphi) \subseteq S(\varphi^r)$ as we only further constrain the set of equations that defines $S(\varphi^r)$ to construct $S(\varphi)$. This leads to some important results for us as if φ^r is not valid then so is φ. This prompts us to think of the different φ as leaves of tree for which internal nodes are restricted φ maps.

More formally, given an order on the points from the Pareto set $\{k_i | i \in [p]\} = p(\mu)$, the root of our tree is the empty map, $\varphi : \varnothing \to [d]$. It has d possible children $\varphi : k_1 \in \{k_1\} \mapsto j$ for all $j \in [d]$. For any of these children $\varphi_1 \in [d]^{\{k_1\}}$, they themselves have d possible children given by $\varphi_2|_{\{k_1\}} = \varphi_1$ and the different possible value for $\varphi_2(k_2)$. We continue this process until all the points are exhausted and the leafs of this tree are the element of $[d]^{[p]}$.

Given this construction and the observation made previously that S is decreasing along the branches of this tree, we propose a recursive backtracking algorithm to enumerate non-empty cells. We start from the root and operate a depth-first search algorithm. When visiting any internal node, we check whether $S(\varphi)$ is empty or not. If it is not empty, we go on with our search until

we hit a leaf yielding a non-empty φ map. Otherwise, we know that any leaves below it will be associated with an empty cell, as such there is no use in visiting this subtree at all and we can backtrack one level up and continue our search in a different subtree.

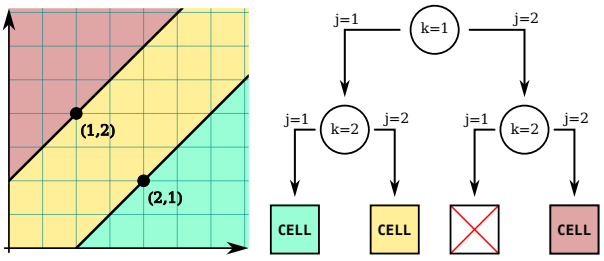

Figure 2: An example of cell construction in 2d with three valid cells and an empty one

Example. Let $\mu_1 = (1, 2)$ and $\mu_2 = (2, 1)$. The root of our tree is the point μ_1 and we try to move it alongside dimension 1 by walking the leftmost edge from the root. There, we check that our linear system still admits solutions

$$\mu_1^1 - \lambda_0^1 \leq \mu_1^2 - \lambda_0^2 \;\Rightarrow\; \lambda_0^2 - \lambda_0^1 \leq \mu_1^2 - \mu_1^1 = 1$$

which it does so we can go on. Now, we add the second point alongside the first coordinate which adds $\lambda_0^2 - \lambda_0^1 \leq \mu_2^2 - \mu_2^1 = -1$ to our set of equations, which still admits a solution. Since this was the last point, this means that $\varphi : 1; 2 \mapsto 1$ was a non-empty cell and we can go on. We now backtrack to try and add the second point alongside the second coordinate. This adds $\lambda_0^1 - \lambda_0^2 \leq \mu_2^1 - \mu_2^2 = 1$ to our set of linear equations. This gives us $-1 \leq \lambda_0^2 - \lambda_0^1 \leq 1$ which admits a solution and thus we found a new non-empty cell. We now backtrack all the way to our root resetting our list of inequalities and we add the first point alongside the second coordinate ($\lambda_0^1 - \lambda_0^2 \leq \mu_1^1 - \mu_1^2 = -1$). But then when we want to add the second point alongside the first coordinate, we end up with the infeasible system $\lambda_0^1 - \lambda_0^2 \leq -1 \wedge \lambda_0^1 - \lambda_0^2 \geq 1$. We can thus discard that sub-tree and backtrack one step. Here the tree has a small depth meaning we are not discarding much, but for a bigger tree it could lead to removing a lot of possible empty cells from our exploration. After that, we continue try to add the second point alongside its second coordinate which leads to a new cell. So in this example, there are four possible φ of which three are a non-empty cell.

Moreover, if we consider the d possible children of a node φ^r (we assume that the mapping of $k \in p(\mu)$ is decided at this point in the tree, and we label φ_j the children), the cell of each φ_j can be obtained by adding constraints to φ^r. If we denote by

$$C_j \triangleq \left\{ \lambda \in \mathbb{R}^d \,\middle|\, \forall j' \in [d],\, \mu_k^j - \lambda^j \leq \mu_k^{j'} - \lambda^{j'} \right\},$$

then $S(\varphi_j) = S(\varphi^r) \cap C_j$. But, since the C_j provide a tesselation of $\mathbb{R}^d$ (a tesselation being a set of closed sets whose union is $\mathbb{R}^d$ and whose interiors are disjoints; it is a partition of the space up to the boundaries of the parts), the $(S(\varphi_j))_{j\in[d]}$ are themselves a tesselation of $S(\varphi^r)$. When iterating this result, we get that, first a valid internal node will have a valid internal child and thus a valid internal leaf within its subtree, and that all (valid) leafs provide a tesselation of $\mathbb{R}^d$ (this is true for any maximal anti-chain of nodes within the tree) since the root has a cell spanning over all of $\mathbb{R}^d$. This will be useful later for bounding the number of valid nodes within the intersection.

The following lemma is proved in Appendix B.

Lemma 4. *Checking whether any node $\varphi^r \in [d]^r$ is valid, i.e. whether its cell $S(\varphi^r)$ is non-empty, can be done in time $O(r + d^3)$. Moreover, by sharing computation we can check each of the d extensions to φ^{r+1} in time $O(d^2)$ each.*

In Appendix C we prove the following upper bound for the number of non-empty cells:

Lemma 5. *The number of cells is bounded by $\binom{p+d-1}{d-1}$ where p is the number of points from the Pareto set.*

3.2.2 Finding the optimum within a cell

We now assume that we reached a leaf of our tree and thus found a valid φ map and we set out to minimize $g_{k_0,\varphi}$ for each different k_0. This means that we fixed the direction in which each point from the Pareto set will move and given this, we want to find the smallest transportation cost to add the point k_0 to the Pareto set. We recall that $g_{k_0,\varphi}$ has the following expression:

$$g_{k_0,\varphi}(\lambda_0) \triangleq \frac{w_0}{2}||\mu_0 - \lambda_0||^2 + \sum_{k\in p(\mu)} \frac{w_k}{2} \left(\mu_k^{\varphi(k)} - \lambda_0^{\varphi(k)}\right)_+^2.$$

Since the $(\varphi^{-1}(j))_{j\in[d]}$ partitions $[K]$, this function can be rewritten as a sum of d different function $(h_j)_{j\in[d]}$ such that h_j only depends on λ_0^j.

$$h_j : \lambda_0^j \in \mathbb{R} \mapsto \frac{w_0}{2}(\mu_0^j - \lambda_0^j)^2 + \sum_{k\in\varphi^{-\infty}(|)} \frac{w_k}{2}(\mu_k^j - \lambda_0^j)_+^2.$$

Thus minimizing each h_j independently is equivalent to minimizing $g_{k_0,\varphi}$. Moreover, each h_j is a strongly differentiable function thus it is minimized at λ_0^{*j} which

is such that $h'_j(\lambda_0^{*j}) = 0$. For the rest of this section, we will assume that $\varphi^{-1}(j) = [p_j]$ and that $\mu_1^j \leq \cdots \leq \mu_{p_j}^j$. We label for $k \in [p_j]$, $x_k = \mu_k^j$ and $x_0 = -\infty, x_{p_j+1} = +\infty$. For $k \in \{0, \cdots, p_j + 1\}$, for $x \in [x_k, x_{k+1}]$,

$$h'_j(x) = w_0(x - \mu_0^j) + \sum_{i=k+1}^{p_j} w_i(x - \mu_i^j) \; .$$

As the function admits a unique minimizer, there is only one $k \in \{0, \cdots, p_j\}$ such that

$$x_k \leq \frac{w_0\mu_0^j + \sum_{i=k+1}^{p_j} w_i\mu_i^j}{w_0 + \sum_{i=k+1}^{p_j} w_i} \leq x_{k+1} \; .$$

The function h_j is minimized at this point and finding this k is done by dynamic programming with $O(p_j)$ operations. This is faster than trying a binary search approach as this would require $O(p_j \log p_j)$ operations. As we need to compute the minimizer of h_j for each j, the computational complexity to add a point to the Pareto set is of order $O(p + d)$. This needs to be done for all non-Pareto optimal points, for a total of $O(K(p + d))$ operations.

We now come back to the assumption we made that the μ_k^j are sorted and filtered with respect to $\varphi^{-1}(j)$. Doing this for each k_0 within each cell would incur a multiplicative cost of $O(p + p_j \log p_j)$. However sorting can be performed prior to building our tree by sorting $(\mu_k^j)_{k\in p(\mu)}$ for each j. This has a cost of $O(dp \log p)$ which is negligible when compared to the rest of our algorithm. Within a cell we can then filter the sorted array to only get $(\mu_k^j)_{k\in\varphi^{-1}(j)}$ sorted in $O(p)$. As this sequence is common for all points k_0 that we might want to add in a cell this doesn't incur a cost every time we would like to add a point to the Pareto front, but just once per cell. This means that for one cell, the complexity to compute the cost to add each point to the Pareto set is $O(pd + K(p + d))$ which is just $O(K(p + d))$. Pulling from Lemma 5 our upper bound on the number of cells, we get that this operation is done at most $\binom{p+d-1}{d-1}$ times, and building the tree yields a final cost of

$$O\left(\left(K(p + d) + pd^3\right)\binom{p + d - 1}{d - 1}\right)$$

as we had set out to prove in Theorem 1.

As most of the settings we aim to tackle can have a large number of arms but only a few dimensions, this algorithmic complexity boils down to $O(Kd^3p^d)$.

We present in Appendix D a speed-up for the dimension two from time $O(Kp^2)$ to time $O(Kp + p \log p)$.

4 EXPERIMENTS

We check the performance of our algorithm against the real-world scenario proposed by [Kone et al., 2023]. We revisit one of their experiment which is based on the study by [Munro et al., 2021] about immunogenicity of a Covid vaccine third dose (see the reference for details on the dataset). The setting is a bandit model ν of $K = 20$ Gaussian arms in dimension $d = 3$ representing three different immunogenicity responses. There are $p(\nu) = 2$ Pareto optimal arms that we need to identify. The means of the arms and the variance of each immunogenicity trait can be found in Appendix E.

For this instance, the instance-dependent factor in the sample complexity lower bound is $T^*(\nu) = 2103.78$. The associated optimal weights are included in Appendix E.

We use a risk of $\delta = 0.1$ and tested the sample complexity average over 2000 runs of the algorithm. Our average sample complexity is 17909. This is significantly lower than the 39000 sample complexity from 0-APE-20 which is the one corresponding to our setting. We use the stylized exploration rate $\beta(t, \delta) = \ln\left(\frac{\ln(1+t)}{\delta}\right)$ as our threshold for the stopping statistic. This is standard in experiments, and though less rigorous than the choice made in [Kone et al., 2023], it is still overly prudent: though the risk parameter δ is set to 0.1, the real risk is much smaller as we obtained no identification mistake over the 2000 runs. This conservative behaviour of pure exploration algorithms has been frequently reported. To speed up the running time of our algorithm, we throttle the number of minimum transportation cost computations. While we perform a gradient ascent step for every sample, we only update the gradient every ten samples and we check the stopping statistic every 25 samples. The experiment took 5 hours to run on 16 (of 20) cores of a dual Intel(R) Xeon(R) CPU E5-2630 v4 machine.

In Figure 3, we show the empirical distribution of the stopping time of our algorithm. We highlight that there is a significative difference between $\mathbb{E}_\theta(\tau_\theta)$ and $\log\left(\frac{1}{\delta}\right) T^*(\theta)$, whereas we could have expected them to be closer to each other. Several factors contribute to this gap. We chose a too large value of δ to exhibit the expected asymptotic behaviour. The analysis shows the presence of a second-order term that is not neglictible on such experiments. It is all the more significant that we chose not to update the gradient at every round but only every few rounds.

This experiment is representative of a real edge of Track-and-Stop in terms of sample complexity. This advantage can be theoretically understood by comparing the complexity bounds when δ goes to 0. For

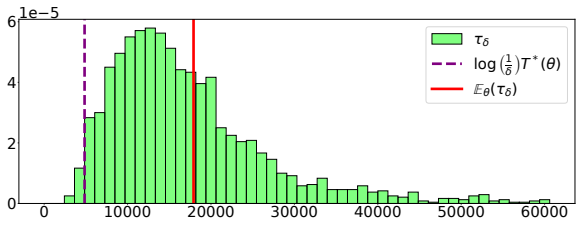

Figure 3: Empirical distribution of the number of samples used to identify the two Pareto optimal points

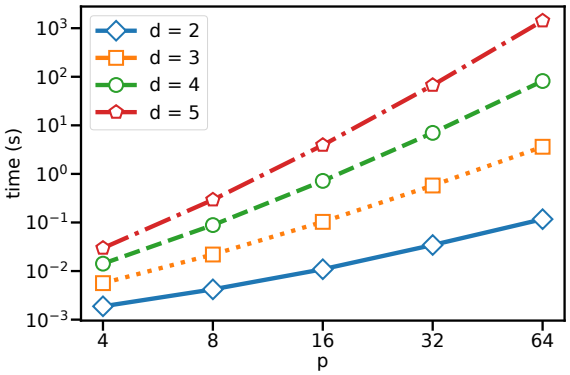

Figure 4: Time to solve the minimization problem on a random point cloud with p Pareto points in dim. d

example, in the scenario when one arm dominates a large number of other identical arms, Track-and-Stop can be proved to be more data efficient by a factor almost 2.

We also ran experiments on random instances to evaluate the computation time of the minimization solver and its dependency on d and p. The random instances on which we ran our algorithm consisted of p points sampled from the all-positive quadrant of a d dimension sphere (as such they are all easily part of the Pareto set) and an additional point at 0. We only ran the minimzation solver of our algorithm on these points and estimated the time it took for each pair of (p, d) on 100 samples. The result of this experiment is represented in Figure 4. In the Figure, we can see that given a fixed d there is a linear dependency between the log of the time taken and the log of the number of point on the Pareto set. The slope of each line is proportional to d. This matches the theorical result obtained in Theorem 1 as for a given d and $K = p + 1$ the complexity of our solver should be $O(p^{d+1})$.

5 CONCLUSION

We tackled the problem of Pareto front identification in a Gaussian multi-armed bandit. To this end, we studied efficient implementation of the core oracle required by the Track-and-Stop framework, namely the gradient of the information-theoretic lower bound. To solve the associated non-convex optimization problem, we split the domain in convex parts, discussed enumerating the parts and solving the convex problem on the parts in closed form.

For future work we are interested in relaxing the assumptions. In particular, we aim to study the problem under dependent coordinates, with Gaussians of unknown variances, in other exponential families, in non-parametric classes, and in the approximate $\epsilon > 0$ case. It would be interesting, challenging and rewarding to pin down the computational complexity of the transportation problem (2), already in the spherical Gaussian case. Can one find and exploit additional structure in the problem to solve it in time at most a fixed and dimension independent degree polynomial in the number of arms K? Or can one prove a lower bound matching Theorem 1?

References

[Agrawal et al., 2021] Agrawal, S., Koolen, W. M., and Juneja, S. (2021). Optimal best-arm identification methods for tail-risk measures. In *Advances in Neural Information Processing Systems (NeurIPS) 34*.

[Al Marjani and Proutiere, 2021] Al Marjani, A. and Proutiere, A. (2021). Adaptive sampling for best policy identification in Markov decision processes. In *International Conference on Machine Learning*, pages 7459–7468.

[Auer et al., 2016] Auer, P., Chiang, C.-K., Ortner, R., and Drugan, M. (2016). Pareto front identification from stochastic bandit feedback. In *Artificial intelligence and statistics*, pages 939–947.

[Busa-Fekete et al., 2017] Busa-Fekete, R., Szörényi, B., Weng, P., and Mannor, S. (2017). Multi-objective bandits: Optimizing the generalized Gini index. In *Proceedings of the 34th International Conference on Machine Learning*, volume 70, pages 625–634.

[Chen et al., 2017a] Chen, J., Chen, X., Zhang, Q., and Zhou, Y. (2017a). Adaptive multiple-arm identification. In *International Conference on Machine Learning*, pages 722–730.

[Chen et al., 2017b] Chen, L., Li, J., and Qiao, M. (2017b). Nearly instance optimal sample complexity bounds for top-k arm selection. In *Artificial Intelligence and Statistics*, pages 101–110.

[Cheu et al., 2018] Cheu, A., Sundaram, R., and Ullman, J. (2018). Skyline identification in multi-arm bandits. In *2018 IEEE International Symposium on Information Theory (ISIT)*, pages 1006–1010.

[Degenne et al., 2019] Degenne, R., Koolen, W. M., and Ménard, P. (2019). Non-asymptotic pure exploration by solving games. In *Advances in Neural Information Processing Systems (NeurIPS) 32*, pages 14492–14501.

[Degenne et al., 2020] Degenne, R., Ménard, P., Shang, X., and Valko, M. (2020). Gamification of pure exploration for linear bandits. In *International Conference on Machine Learning*, pages 2432–2442.

[Erickson, 2019] Erickson, J. (2019). *Algorithms*. Jeff Erickson.

[Garivier and Kaufmann, 2016] Garivier, A. and Kaufmann, E. (2016). Optimal best arm identification with fixed confidence. In *29th Annual Conference on Learning Theory*, volume 49 of *Proceedings of Machine Learning Research*, pages 998–1027.

[Garivier et al., 2016] Garivier, A., Kaufmann, E., and Koolen, W. M. (2016). Maximin action identification: A new bandit framework for games. In *Proceedings of the 29th Annual Conference on Learning Theory (COLT)*, pages 1028 – 1050.

[Garivier et al., 2017] Garivier, A., Ménard, P., and Rossi, L. (2017). Thresholding bandit for dose-ranging: The impact of monotonicity. *arXiv preprint arXiv:1711.04454*.

[Haddenhorst et al., 2021] Haddenhorst, B., Bengs, V., and Hüllermeier, E. (2021). Identification of the generalized Condorcet winner in multi-dueling bandits. *Advances in Neural Information Processing Systems*, 34:25904–25916.

[Hao et al., 2020] Hao, B., Lattimore, T., and Szepesvári, C. (2020). Adaptive exploration in linear contextual bandit. In *International Conference on Artificial Intelligence and Statistics*, pages 3536–3545.

[Jedra and Proutiere, 2020] Jedra, Y. and Proutiere, A. (2020). Optimal best-arm identification in linear bandits. *Advances in Neural Information Processing Systems*, 33:10007–10017.

[Katariya et al., 2019] Katariya, S., Tripathy, A., and Nowak, R. (2019). Maxgap bandit: Adaptive algorithms for approximate ranking. *Advances in Neural Information Processing Systems*, 32.

[Kocák and Garivier, 2021] Kocák, T. and Garivier, A. (2021). Epsilon best arm identification in spectral bandits. In *IJCAI*, pages 2636–2642.

[Kone et al., 2023] Kone, C., Kaufmann, E., and Richert, L. (2023). Adaptive algorithms for relaxed Pareto set identification. *arXiv preprint arXiv:2307.00424*.

[Moulos, 2019] Moulos, V. (2019). Optimal best Markovian arm identification with fixed confidence. *Advances in Neural Information Processing Systems*, 32.

[Munro et al., 2021] Munro, A. P. S., Janani, L., and et al (2021). Safety and immunogenicity of seven covid-19 vaccines as a third dose (booster) following two doses of chadox1 ncov-19 or bnt162b2 in the uk (cov-boost): a blinded, multicentre, randomised, controlled, phase 2 trial. *The Lancet*, 398(10318):2258–2276.

[Russac et al., 2021] Russac, Y., Katsimerou, C., Bohle, D., Cappé, O., Garivier, A., and Koolen, W. M. (2021). A/B/n testing with control in the presence of subpopulations. In *Advances in Neural Information Processing Systems (NeurIPS) 34*.

[Schrijver, 2003] Schrijver, A. (2003). *Combinatorial optimization: polyhedra and efficiency*. Springer.

[Tirinzoni et al., 2020] Tirinzoni, A., Pirotta, M., Restelli, M., and Lazaric, A. (2020). An asymptotically optimal primal-dual incremental algorithm for contextual linear bandits. *Advances in Neural Information Processing Systems*, 33:1417–1427.

[Wang et al., 2021] Wang, P.-A., Tzeng, R.-C., and Proutière, A. (2021). Fast pure exploration via Frank-Wolfe.

[Xu and Klabjan, 2023] Xu, M. and Klabjan, D. (2023). Pareto regret analyses in multi-objective multi-armed bandit. In *Proceedings of the 40th International Conference on Machine Learning*, volume 202, pages 38499–38517.

[Zuluaga et al., 2013] Zuluaga, M., Sergent, G., Krause, A., and Püschel, M. (2013). Active learning for multi-objective optimization. In Dasgupta, S. and McAllester, D., editors, *Proceedings of the 30th International Conference on Machine Learning*, volume 28 of *Proceedings of Machine Learning Research*, pages 462–470, Atlanta, Georgia, USA. PMLR.

Checklist

1. For all models and algorithms presented, check if you include:
   (a) A clear description of the mathematical setting, assumptions, algorithm, and/or model. Yes
   (b) An analysis of the properties and complexity (time, space, sample size) of any algorithm. Yes
   (c) (Optional) Anonymized source code, with specification of all dependencies, including external libraries. Yes
2. For any theoretical claim, check if you include:
   (a) Statements of the full set of assumptions of all theoretical results. Yes
   (b) Complete proofs of all theoretical results. Yes
   (c) Clear explanations of any assumptions. Yes
3. For all figures and tables that present empirical results, check if you include:
   (a) The code, data, and instructions needed to reproduce the main experimental results (either in the supplemental material or as a URL). Yes
   (b) All the training details (e.g., data splits, hyperparameters, how they were chosen). Not Applicable
   (c) A clear definition of the specific measure or statistics and error bars (e.g., with respect to the random seed after running experiments multiple times). Yes
   (d) A description of the computing infrastructure used. (e.g., type of GPUs, internal cluster, or cloud provider). Yes
4. If you are using existing assets (e.g., code, data, models) or curating/releasing new assets, check if you include:
   (a) Citations of the creator If your work uses existing assets. Not Applicable
   (b) The license information of the assets, if applicable. Not Applicable
   (c) New assets either in the supplemental material or as a URL, if applicable. Not Applicable
   (d) Information about consent from data providers/curators. Not Applicable
   (e) Discussion of sensible content if applicable, e.g., personally identifiable information or offensive content. Not Applicable
5. If you used crowdsourcing or conducted research with human subjects, check if you include:
   (a) The full text of instructions given to participants and screenshots. Not Applicable
   (b) Descriptions of potential participant risks, with links to Institutional Review Board (IRB) approvals if applicable. Not Applicable
   (c) The estimated hourly wage paid to participants and the total amount spent on participant compensation. Not Applicable

A Proof of Lemma 1: Splitting the domain

Proof of Lemma 1. $\implies$) We assume $p(\mu) \neq p(\lambda)$. Then either $p(\mu)\backslash p(\lambda)$ or $p(\lambda)\backslash p(\mu)$ is not empty. We assume the first for now. And we let $k_0 \in p(\mu)\backslash p(\lambda)$. Since $k_0 \notin p(\lambda)$, then its set of dominators in λ is not empty. If any of its dominators in λ belongs to $p(\mu)$, then we have found $k_0, k_1 \in p(\mu)$ such that $k_0 \preceq_\lambda k_1$. Otherwise let k_0' from k_0's set of dominators in λ since it is not empty. We know that k_0' does not belong to $p(\mu)$ and since all of its dominators in λ is included in k_0's one (by transitivity), then none of its dominators belongs to $p(\mu)$. Thus, we found $k_0' \notin p(\mu)$ such that it is not dominated in λ by any point from $p(\mu)$.

We now assume that $p(\lambda)\backslash p(\mu)$ is not empty. Then there exists $k_0 \in p(\lambda)$ such that $k_0 \notin p(\mu)$. Let k_0 be such an index and since it belongs in $p(\lambda)$ no one dominates it and in particular points from $p(\mu)$.

$\impliedby$) We first assume that there exists $k_0, k_1 \in p(\mu)$ such that $k_0 \preceq_\lambda k_1$. Let k_0, k_1 such indices. Since $k_0 \preceq_\lambda k_1$ then $k_0 \notin p(\lambda)$. Hence $p(\mu) \neq p(\lambda)$.

We now assume that there exists $k_0 \notin p(\mu)$ such that no points in $p(\mu)$ dominates it in λ. Let k_0 such an index. Either k_0 is now on the Pareto set and we are done or there exists a point k from the Pareto set of λ that dominates it. But then this point is not within $p(\mu)$ (because no points in from $p(\mu)$ dominates k_0 in λ) and is in $p(\lambda)$. Hence $p(\mu) \neq p(\lambda)$. □

B Proof of Lemma 4: An efficient algorithm for our linear system of equations

To check whether our system of equations admits a solution, we could invoke a linear programming solver to get an answer. Here we leverage the particular structure of our set of inequalities to decide feasibility more efficiently. First note that any of the inequalities that we might add to our system is of the form $\lambda_0^{j_2} - \lambda_0^{j_1} \leq \mu_k^{j_2} - \mu_k^{j_1}$. Thus our system of inequalities might be viewed as a sequence of upper bounds for differences of coordinates of λ_0. To check whether this system admits a solution we introduce a directed multi-graph G with nodes labeled by the $j \in [d]$. For each constraint of the form $\lambda_0^{j_2} - \lambda_0^{j_1} \leq \mu_k^{j_2} - \mu_k^{j_1}$ we add an edge going from j_1 to j_2 which has value $\mu_k^{j_2} - \mu_k^{j_1}$. We use a multi-graph representation because it has a one to one mapping with our system of equation.

We recall a well-known [Erickson, 2019] equivalence between the existence of a solution for a set of equations that can be encoded thusly.

Lemma 6. *Let $G = (V, E)$ be a finite directed graph where $E \subseteq VV\mathbb{R}$. The system*

$$\lambda \in \mathbb{R}^d \quad s.t. \quad \forall (i, j, v) \in E : \lambda_i - \lambda_j \leq v$$

has a solution iff G has no negative cycle.

Proof. We assume that G contains a negative cycle $j_0 \to_{v_1} \cdots \to_{v_n} j_n = j_0$. Then, we know that for all $i \in [n]$ the equation $\lambda_{j_i} - \lambda_{j_{i-1}} \leq v_i$ is present in our linear system. Summing these inequalities gives us

$$0 = \lambda_{j_n} - \lambda_{j_0} = \sum_{i \in [d]} \lambda_{j_i} - \lambda_{j_{i-1}} \leq \sum_{i \in [d]} v_i < 0 \,.$$

Hence our system does not admit solutions.

Now we assume that the graph doesn't contains a negative cycle and we introduce a source point s which we connect to every vertex of G with an edge of length 0. This updated graph still doesn't contain negative cycles because no new cycles have been created. Thus we can define $\delta : j \in [d] \to \mathbb{R}$ the function that gives the length of the shortest path from s to j. We claim that setting λ_0^j to $\delta(j)$ respects every inequality and thus is a solution to our linear system of equations. This is due to the fact that for every edge $j_1 \to_v j_2$ the triangular inequality gives us that $\delta(j_2) \leq \delta(j_1) + v$. □

As such, we could, at each internal node of our tree, create the graph associated with the set of equations encountered so far and check the presence of negative cycles. If there are any we backtrack, otherwise we go on. If we do that, to check for presence of negative cycle we don't have a much better choice than the Bellman-Ford algorithm [Schrijver, 2003] because of the presence of negative edges. This would yield a algorithmic complexity of $O(VE)$ which in our case more often than not would look like d^3. We can reduce that to a d^2 by noting that

when we make our choice of (k, j) when going down the tree, the graph at the parent and the child node only differ by a few edges, the one stemming from node j. Thus if we already know the shortest path in the original graph (which is assumed to not contain negative cycles), we can leverage that knowledge to speed up our negative cycle detection at the child node, which we state in the next lemma.

Lemma 7. *Let $G = (V, E)$ a directed weighted graph with no negative cycles and such that $v : VV \to \mathbb{R}$ is the length of the shortest path between every pair of points. Let $\{u_x\}_{x\in V}$ some new edges between 0 and x such that $G' = (V, E \cap \{u_x\}_{x\in V})$. Negative cycle detection and updated shortest paths can be performed in time $O(d^2)$.*

Proof. If the graph G' now contains a negative cycle, it is going through an updated edge as G doesn't contain a negative cycle. By induction the minimal value of a cycle going from and back to 0 without visiting any other nodes more than once is $\min_{x\neq 0} u_x + s(x, 0)$ where $s(x, y)$ is the length of the shortest simple path (a path that never goes twice through the same vertex) from x to y in G'. But that simple path from x to 0 don't go through any updated edge, hence $s(x, 0) = v(x, 0)$. Thus if all $u_x + v(x, 0) \geq 0$ there is no negative cycle in our updated graph and if any $u(x) + v(x, 0)$ is negative, we found a negative cycle. This can be checked in $O(d)$.

We now assume that there is no negative cycle in G' and set out to compute $s(x, y)$ for all $x, y \in V$. First as stated earlier, paths that go to 0 haven't changed cost as they cannot go through any of the updated edges. We now update edges going from 0 and claim that $s(0, x) = \min B$ where $B = \{{}_y u_y + v(y, x) \,|\, y \in V\} \cup \{v(0, x)\}$.

First, we show that $s(0, x) \in B$. Let $p = 0 \to_{e_1} y^* \to \cdots \to x$, then either e_1 is an edge that was present in G and thus $s(0, x) = v(0, x)$ or e_1 was not and then it has weight u_{y^*}. We call l the length of the path $x \to \cdots \to y^*$ in G'. Since the path p is the shortest between 0 and x and that there is no negative cycle, the part of p between y^* and x doesn't go through 0 and as such any new edges. Since it is the shortest path between y^* and x and it stays in common part of G and G', we get that $l = v(y, x)$. Hence the length of this path is $u_{y^*} + v(y^*, x)$.

The shortest path between 0 and x in G is still a path in G' thus $s(0, x) \leq v(0, x)$. Now for all $y \in V$, either the shortest path from y to x in G' doesn't goes though 0 or it goes through it. In the first case, the path $0 \to y \to \cdots \to x$ in G' has value $u_y + v(y, x)$ and since it is the length of a path from 0 to x, we know that $s(0, x) \leq u(y) + v(y, x)$. In the second case, we know that the shortest path from y to x in G' goes exactly once through 0 (otherwise there would be a negative cycle), and using the optimality of subpath, we know that the part of the path from y to x after going through 0 is the shortest path between 0 and x, thus the next point visited is y^* and this part of the path has length $s(0, x)$, which is such that $s(0, x) \leq v(0, x)$. Similarly since the part between y and 0 is the shortest path between these points in G' and that it doesn't go through an edge stemming from 0, we know that it has length $v(y, 0)$ giving us the final length from this path to be $u(y) + v(y, 0) + s(0, x)$. Since there is no negative cycles we know that $u(y) + v(y, 0) \geq 0$. Since all path from y to x in G are still path in G' we have that $v(y, 0) + s(0, x) = s(y, x) \leq v(y, x)$. This gives us that

$$s(0, x) \leq u(y) + v(y, 0) + s(0, x) \leq u(y) + v(y, x) \ .$$

Hence for all $b \in B$, $b \geq s(0, x)$ and $s(0, x) \in B$, which give us that $s(0, x) = \min B$. Hence all shortest path from 0 to other nodes can be updated in $O(d^2)$.

To conclude, we only need to update all distances going neither from nor to 0. We claim that for x and y which are not 0, $s(x, y) = \min\{v(x, y)s(x, 0) + s(0, y)\}$. First, we highlight that $s(x, 0) + s(0, y)$ is the length of the shortest path from x to y going through 0 in G' and that $v(x, y)$ is the length of the shortest path from x to y in G which is still present in G'. Thus both of them are path length in G' from x to y and we just need to show that either of them has an optimal length. The shortest path from x to y in G' either goes through an edge stemming from 0 or it doesn't. In the first case, it has value $v(x, y)$ otherwise it has value $s(x, 0) + s(0, y)$. Hence $s(x, y) = \min\{v(x, y); s(x, 0) + s(0, y)\}$. All these distances can be updated in $O(d^2)$ which concludes our proof. □

C Proof of Lemma 5: Counting cells

As stated earlier, the number of possible φ maps is d^p but of these, quite a lot don't lead to a cell. To better estimate the complexity of our algorithm, we would like, with p and d known, to give a tighter estimate of the number of cells. In this section, we start by showing for small dimensions how to derive explicitly the number of cells. Then we provide an upper bound for arbitrary dimension.

Dimension 1: Though it might feel a bit dull, we will start by tackling the case of best arm identification. As there is only one dimension to choose from, the number of cells is exactly one.

For higher dimensions, we first start by noting that cells are invariant to translation by the all-ones vector, as adding the same offset to λ_0^j in every dimension will not change the comparison between the $\mu_k^j - \lambda_0^j$ for different j. Thus, even though cells live in $\mathbb{R}^d$, they can be reduced to the orthogonal space of the all-ones vector which has dimension $d-1$.

In **dimension 2**, the direction toward which a point μ_k should go are given by whether λ_0 is above or below the diagonal line stemming from μ_k. In the reduced space this is equivalent to being right or left of the projected μ_k. As such there is $p+1$ different cells: one to the right of every point, one to the left of the rightmost point and one to the right of all the other points and so on until all points are on the left.

In **dimension 3**, all points shatter the space (original and reduced) in three distinct parts: one where the distance to the first, second or third dimension is the smallest. In the reduced space, they are delimited by three lines stemming from the projected point and going to infinity. Using this representation (shown in Figure 5, it is possible to use Euler's formula to count the number of different cells. To do so, we will count the number of cells iteratively by adding the μ_k one by one. We start with no points, which means we have 1 cell, 0 edges and 0 vertices. When we add the $k+1^{\text{th}}$ point, for all the previously added points, one of its edge will cross one of the previously added edges adding 1 point and 2 edges per point. This makes the total number of edges and vertices added by adding a new point be $3+2k$ for the edges and $1+k$. Using Euler's formula, we get that the number of added cells is given by $3+2k-(k+1)=k+2$. Hence the number of cells for k points in the Pareto set is

$$1+\sum_{i=1}^{k}(i-1)+2=\frac{k(k+1)}{2}\,. \tag{7}$$

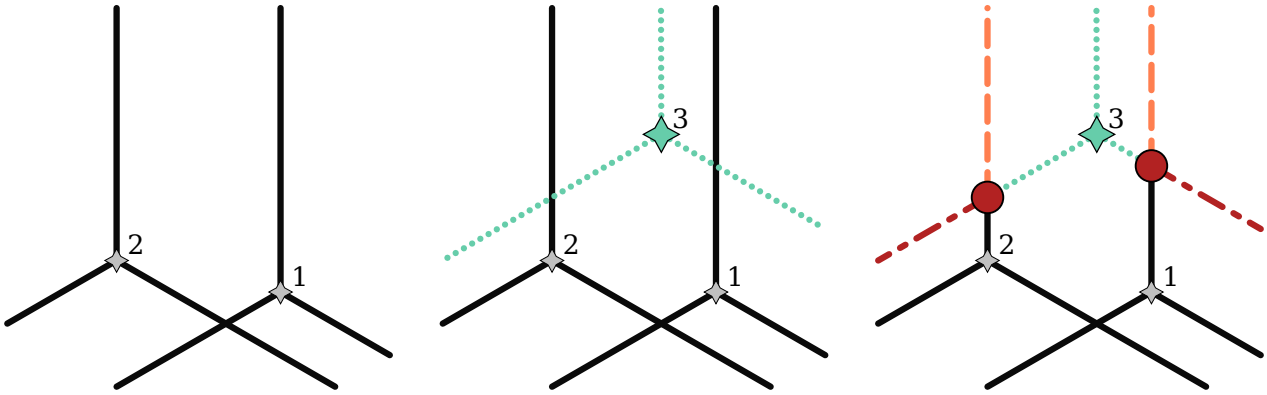

(a) Initial setting with two points.

(b) An additional third point is added, adding a vertex and three edges.

(c) For every previously added point, one of the added edges intersects with an old edge adding one vertex and two edges.

Figure 5: Example of a point being added in dimension 3

Proof of Lemma 5. To show this lemma, we reuse our graph representation from the previous section. For a specific (j_1, j_2), the list of edges going from j_1 to j_2 in our multi graph G is given by $\{\mu_k^{j_2} - \mu_k^{j_1} \,|\, k \in \varphi^{-\infty}(|)\}$ and for a specific node k such that $j_1 = \varphi(k)$ an edge is created between j_1 and every other $j_2 \neq j_1 \in [d]$ with value $\mu_k^{j_2} - \mu_k^{j_1}$.

First, let $v(\varphi) = \big(\text{Card}(\varphi^{-1}(j))\big)_{j\in[d]}$. We want to show that for a specific value of $v(\varphi)$, there is at most one possible φ which leads to a valid cell. To do that, we show that for φ, φ' such that $v(\varphi) = v(\varphi')$, there exists a particular permutation π such that $\varphi' = \varphi \circ \pi$. Then we show that if there were no negative cycles in G, the multi-graph associated with φ, then the transformation of G to G' after having applied the permutation creates a negative cycle. We conclude by saying that the cardinality of the image of v is $\binom{p+d-1}{d-1}$.

Let φ, φ' such that $v(\varphi) = v(\varphi')$ but $\varphi \neq \varphi'$. For each $j \in [d]$ we let $\pi_j : \varphi'^{-1}(j) \to \varphi^{-1}(j)$ be a bijection between its domain and its image (there exists one since they have the same cardinal $v(\varphi)_j = v(\varphi')_j$). We now define $\pi : k \in p(\mu) \to \pi_{\varphi'(k)}(k)$. Let k_0, k_1 such that $\pi(k_0) = \pi(k_1)$, since the $\varphi^{-1}(j)$ we know that there exists a unique j such that $\pi(k_0) \in \varphi^{-1}(j)$, thus $k_0, k_1 \in \varphi'^{-1}(j)$ and $\pi_j(k_0) = \pi_j(k_1)$ but since π_j is a bijection between $\varphi'^{-1}(j)$ and $\varphi^{-1}(j)$ we get that $k_0 = k_1$. Hence π is injective. And since π's domain and image has the same cardinal, it is bijective. Now, for all $k \in p(\mu)$ with $j = \varphi'(k)$, $\pi(k) \in \varphi^{-1}(j)$ hence $\varphi \circ \pi(k) = j = \varphi'(k)$. Thus, for all φ, φ' such that $v(\varphi) = v(\varphi')$ there exists a permutation π such that $\varphi' = \varphi \circ \pi$.

We now decompose π in disjoints cycles. If a cycle $c = (k_1, \cdots, k_n)$ is such that $\varphi(k_1) = \cdots = \varphi(k_n)$ then this cycle can be omitted from the permutation and it would yield the same φ'. If all cycles were to be removed this way, we would end up with $\varphi = \varphi' \circ Id = \varphi'$, thus we can conclude that at least one cycle as to be such that $\mathrm{Card}\,(\varphi\{k_1, \cdots, k_n\}) > 1$. We now restrict ourselves to π with only such cycles as other can be safely deleted without changing the resulting φ'. We now focus on a cycle $c = (k_1, \cdots, k_n)$ such that there exists $x < y \in [n]$ such that $\varphi(k_x) = \varphi(k_y)$ and we prove that there exists two cycles c_x, c_y by which c can be replaced in π which yields the same φ'. Since $\varphi(k_x) = \varphi(k_y)$ then $\varphi \circ \pi = \varphi \circ (k_x k_y) \circ \pi$, and $(k_x k_y) \circ \pi$ is permutation that has the same cycle than π except for c which has been split in two disjoints cycles (they are disjoint from each other and from cycles in π which are not c): $c_x = (k_x, \cdots, k_{y-1})$ and $c_y = (k_y, \cdots, k_{x-1})$. Thus π and $(k_x k_y) \circ \pi$ yield the same φ', and we can restrict ourselves to permutation such that all $\varphi(k_i)$ are distinct within each different cycle.

We let π be such a permutation and we introduce G, the multi-graph associated with φ and G' the one for $\varphi' = \varphi \circ \pi$. We now assume that φ is a valid map and we will restrict the rest of our study on the changes operated on G by a specific cycle $c = (k_i)_{i \in [n]}$. Let $i \in [n], j_1 = \varphi(k_i)$ and $j_2 = \varphi'(k_i) = \varphi(k_{i+1})$. Since $j_1 \neq j_2$, we know that there exists an edge in G between j_1 and j_2 of value $v_i \triangleq \mu^{j_2}_{k_i} - \mu^{j_1}_{k_i}$, respectively in G' we know that there is an edge between j_2 and j_1 of value $\mu^{j_1}_{k_i} - \mu^{j_2}_{k_i} = -v_i$. As φ is assumed to be a valid map, the cycle from G

$$\varphi(k_1) \to_{v_1} \cdots \to_{v_{n-1}} \varphi(k_n) \to_{v_n} \varphi(k_1)$$

is not negative. As such, the cycle from G' given by

$$\varphi'(k_n) \leftarrow_{-v_1} \varphi'(k_1) \leftarrow_{-v_2} \cdots \leftarrow_{-v_n} \varphi'(k_n)$$

is a negative cycle. Thus there is at most one valid map for every point of the image of v.

The image of v is the set of vectors of length d whose entries are natural numbers that sum to p. It is a well-known result that this set has cardinality $\binom{p+d-1}{d-1}$, which concludes the proof. □

We believe that this bound is in fact the exact cell count (as seen for dimensions up to 3, cf Eq.7 and by simulations for p, d up to 11) but we settle for this upper bound in the analysis of the complexity. What this tells us is that the number of leaves within the tree is at most $\binom{p+d-1}{d-1}$. Using the observation that if an internal node is not empty there always exists a non-empty leaf below it, we know that the number of valid internal nodes at a given depth is bounded by $\binom{p+d-1}{d-1}$. Thus, the number of non-empty internal nodes is bounded by $p\binom{p+d-1}{d-1}$. Each of these non-empty internal nodes may have at most d children which can be non-empty or empty internal or non-empty or empty leaves. As we run our cell elimination procedure for each child of each non-empty internal node, we run our procedure at most $dp\binom{p+d-1}{d-1}$ times. Since this procedure has complexity d^2 we end up with a complexity of $d^3 p\binom{p+d-1}{d-1}$ to construct our tree.

D Speed-up for Dimension 2

In this section we present a speed-up in run time available for dimension $d = 2$. The transportation cost computations both for removing a point from the front and for adding a point to the front are presented next.

D.1 Removing a point

We present an update of Lemma 2 for dimension 2. Here, we can leverage the geometry of our problem to disregard most of the pairs (k_0, k_1). Let's assume that we are considering the pair (k_0, k_2) and that there exists an arm k_1 in the Pareto set between k_0 and k_2 (i.e. $\mu^1_{k_0} \geq \mu^1_{k_1} \geq \mu^1_{k_2}$ and $\mu^2_{k_0} \leq \mu^2_{k_1} \leq \mu^2_{k_2}$). Now the inf reached at $\lambda^1_{k_0} = \lambda^1_{k_2}$ will be either above or below $\mu^1_{k_1}$. If it is reached below then $\mu^1_{k_1} = \lambda^1_{k_1} \geq \lambda^1_{k_0}$ which means the cost

of shadowing k_0 with k_2 is higher than the cost of shadowing k_0 with k_1 and if it is above then $\mu^1_{k_1} = \lambda^1_{k_1} \leq \lambda^1_{k_2}$ which means the cost of shadowing k_0 with k_2 is higher than the cost of shadowing k_1 with k_2. Hence by ordering the Pareto set, we can restrict ourselves to only look at adjacent points within the Pareto set as these will yield the smallest transportation cost. This means that the number of pair that we need to examine is just $O(p)$ giving us the reduced computation cost $O(p)$ for removing a point.

However, this technique doesn't scale well with higher dimensions. Given three points (k_0, k_1, k_2), a similar result can be obtained if there exists j_a such that $\mu^{j_a}_{k_0} \geq \mu^{j_a}_{k_2} \geq \mu^{j_a}_{k_1}$ and for all $j \neq j_a$, $\mu^j_{k_0} \leq \mu^j_{k_2} \leq \mu^j_{k_1}$. In this setting the minimizer λ of the transportation cost to shadow k_0 by k_1 is such that either $\lambda^{j_a}_{k_0} \leq \mu^{j_a}_{k_2}$ and then $\lambda_{k_0} \preceq \mu_{k_2}$ or $\lambda^{j_a}_{k_1} (= \lambda^{j_a}_{k_0}) \geq \mu^{j_a}_{k_2}$ and then $\mu_{k_2} \preceq \lambda_{k_1}$. As previously, we found that computing the value for the pair k_0, k_1 was unnecessary because either the pair (k_0, k_2) or (k_2, k_1) would have yielded a smaller value. But this was done in a pretty constrained way, removing the constraint that there is at most one direction alongside which $\mu^j_{k_0} \geq \mu^j_{k_1}$ won't lead to any results. To see that, let j_a, j_b such that $\forall j \in \{j_a, j_b\}$, $\mu^j_{k_0} \geq \mu^j_{k_2} \geq \mu^j_{k_1}$, then we might end up with $\lambda^{j_a}_{k_0} \leq \mu^{j_a}_{k_2}$ and $\lambda^{j_b}_{k_0} \geq \mu^{j_b}_{k_2}$, leading to no claim of the shape $\lambda_{k_0} \preceq \mu_{k_2}$ or $\mu_{k_2} \preceq \lambda_{k_1}$.

D.2 Adding a point

Here we present an update of Lemma 3 for dimension 2. Again, the geometry of the Pareto front allows us to speed up the computation of the minimal transportation cost to add a point to the Pareto set.

We recall the definition of the function g_{k_0} which, given a new location λ_0 for the point μ_{k_0} (labeled μ_0 for ease of notation) gives the smallest transportation cost to add this point to the Pareto set while moving it to the new location.

$$g_{k_0}(\lambda_0) = \frac{w_0}{2}||\mu_0 - \lambda_0||^2 + \sum_{k \in p(\mu)} \frac{w_k}{2} \min_{j \in [d]} \left(\mu^j_k - \lambda^j_0\right)^2_+ .$$

And given a map $\varphi : p(\mu) \to [d]$, we also recall the function

$$g_{k_0,\varphi}(\lambda_0) = \frac{w_0}{2}||\mu_0 - \lambda_0||^2 + \sum_{k \in p(\mu)} \frac{w_k}{2} \left(\mu^{\varphi(k)}_k - \lambda^{\varphi(k)}_0\right)^2_+ .$$

The functions g_{k_0} and $g_{k_0,\varphi}$ are equal on a set $S(\varphi)$ which consists of the solutions of the following linear system:

$$\lambda_0 \in \mathbb{R}^d \text{ st. } \forall k \in p(\mu),\, \forall j \in [d],\, \mu^{\varphi(k)}_k - \lambda^{\varphi(k)}_0 \leq \mu^j_k - \lambda^j_0$$

and outside of this set, $g_{k_0} \leq g_{k_0,\varphi}$. We highlight here that for any $\lambda_0 \in S(\varphi)$, the line generated by $\lambda_0 + t\mathbb{1}$ is included in $S(\varphi)$ where $\mathbb{1}$ consists of the all-one vector. Hence the geometry of cells can be reduced to the orthogonal space to $\mathbb{R}\mathbb{1}$. Thus from now on, we will decompose λ_0 in an s part which lives in $\mathbb{R}^{d-1}$ and a t part which lives in $\mathbb{R}$, such that $\lambda_0 = Ms + t\mathbb{1}$, where M is a $dd-1$ matrix such that its columns are all orthogonal to each others and to $\mathbb{1}$, and of norm 1. We apply the analogous decomposition to μ_0 and $(\mu_k)_{k \in p(\mu)}$ leading to s_0, t_0 and $(s_k, t_k)_{k \in p(\mu)}$ and we redefine the functions g_{k_0} and $g_{k_0,\varphi}$ accordingly:

$$g_{k_0,\varphi}(s,t) = \frac{w_0}{2}\left(||s_0 - s||^2 + d(t_0 - t)^2\right) + \sum_{k \in p(\mu)} \frac{w_k}{2} \left((M(s_k - s))_{\varphi(k)} + t_k - t\right)^2_+ .$$

For a given s and φ, we are interested in finding the t that minimizes $g_{k_0,\varphi}(s,t)$. We label $t^*_\varphi(s)$ and $g_{k_0,\varphi}(s)$ (resp. $t^*(s)$ and $g_{k_0}(s)$ for the minimizer and the minimal value of $g_{k_0}(s,t)$ with respect to t).

Now that we introduced this reparametriaztion of the problem, we want to show that the function $t^*(s)$ is piecewise linear and that in dimension $d = 2$ it is possible to enumerate its pieces and minimize g_{k_0} with a lower complexity than before.

In dimension 2, the constraints on matrix M leaves us only two choice: either $\begin{bmatrix} -\frac{1}{\sqrt{2}} & \frac{1}{\sqrt{2}} \end{bmatrix}$ or $\begin{bmatrix} \frac{1}{\sqrt{2}} & -\frac{1}{\sqrt{2}} \end{bmatrix}$. We can pick either without loss of generality. We settle for $\begin{bmatrix} \frac{1}{\sqrt{2}} & -\frac{1}{\sqrt{2}} \end{bmatrix}$. We assume for the rest of this section that $s_1 \leq \cdots \leq s_k$

It is also possible to enumerate the valid φ maps in dimension 2. There are $p+1$ different cells given by: $(-\infty, s_1], [s_1, s_2], \cdots, [s_{p-1}, s_p], [s_p, +\infty)$. And the φ map associated with the l^{th} cell of this list is

$$\varphi : k \in p(\mu) \mapsto \begin{cases} 2 & \text{if } k < l \\ 1 & \text{otherwise} \end{cases}.$$

This is due to the fact that $M(s_k - s) = \frac{1}{\sqrt{2}}(s_k - s)\begin{bmatrix} 1 & -1 \end{bmatrix}$. So when $s \leq s_k$, $M_2(s_k - s) \leq M_1(s_k - s)$ and $M_1(s_k - s) \leq M_2(s_k - s)$ when $s \geq s_k$.

We let $t_{k,\varphi} : s \mapsto M_{\varphi(k)}(s_k - s)) + t_k$. It is a linear function of s.

Lemma 8. *The function $t_k(\cdot)$ such that $\forall \varphi$, $\forall x \in S(\varphi)$, $t_k(s) = t_{k,\varphi}(s)$ is well-defined and piecewise linear of slope $\frac{1}{\sqrt{2}}$ before s_k and $-\frac{1}{\sqrt{2}}$ after.*

Proof. Since the $S(\varphi)$ provide a tesselation of the space, we only need to check that given two maps φ_1 and φ_2, the value at the intersection of their cell boundaries is equal. The only points at which cells have a non empty intersect are the s_k's. These cells are associated with the map φ_1 that maps every index stricly below k to 2 and the other ones to 1 and φ_2 the one that maps every index below or equal to k to 2 and the other ones to 1. But $t_{k,\varphi_1}(s_k) = t_k = t_{k,\varphi_2}(s_k)$, hence $t_k(\cdot)$ is well defined and on each of the $S(\varphi)$ it is linear thus it is piecewise linear. Moreover, using the cells described earlier, we have that for $s < s_k$ (resp. $s > s_k$), the φ map associated with the cell in which s lives maps k to 2 (resp. 1), thus $t_k(\cdot)$ is linear on $s \leq s_k$ (resp. $s \geq s_k$) with slope $\frac{1}{\sqrt{2}}$ (resp. $-\frac{1}{\sqrt{2}}$). □

The Figure 6 gives an example of a construction of t^* and the $t_k(\cdot)$. The red dashed line represent here each individual $t_k(\cdot)$ where we can easily see the increasing part up to s_k followed by a decreasing part.

Lemma 9. *t^*_φ and t^* are well-defined and piecewise linear.*

Proof. $g_{k_0,\varphi}$ is differentiable hence, t^*_φ is such that $\frac{\partial g_{k_0,\varphi}}{\partial t}(s, t^*_\varphi(s)) = 0$. The partial derivative of $g_{k_0,\varphi}$ with respect to its second argument is

$$\frac{\partial g_{k_0,\varphi}}{\partial t}(s,t) = dw_0(t - t_0) + \sum_{k \in p(\mu)} w_k (t - t_{k,\varphi}(s))_-$$

Since $g_{k_0,\varphi}(s,\cdot)$ is strongly convex it admits exactly one minimizer, thus, there exists $t^*_\varphi(s)$ such that $t^*_\varphi(s)$ is the minimizer of $g_{k_0,\varphi}$. However, the negative part in the sum makes it so we cannot solve easily for $\frac{\partial g_{k_0,\varphi}}{\partial t}(s, t^*_\varphi(s)) = 0$. But, since $g_{k_0,\varphi}$ is convex, t^*_φ is continuous and then $K(s) \triangleq \mathbb{1}\{t^*_\varphi(\cdot) \leq t_{k,\varphi}(\cdot)\}$ is piecewise constant and only jumps when t^*_φ meets one of the $t_{k,\varphi}$. Thus, if we know $K(s)$ and $t^*_\varphi(s)$ is different from all the $t_{k,\varphi}(s)$ we can differentiate t^*_φ in s giving us the following expression:

$$\frac{\partial t^*_\varphi}{\partial s}(s) = -\frac{\sum_{k \in K(s)} w_k M_{\varphi(k)}}{dw_0 + \sum_{k \in K(s)} w_k}$$

which is constant while $K(s)$ stays the same, meaning that $t^*_\varphi(s)$ is actually piecewise linear. Also its slope is always in $(-\frac{1}{\sqrt{2}}, \frac{1}{\sqrt{2}})$.

t^* is equal to t^*_φ on $S(\varphi)$ meaning that t^* is also piecewise linear and witth slopes in $(-\frac{1}{\sqrt{2}}, \frac{1}{\sqrt{2}})$. This means that t^* will only meet $t_k(\cdot)$ twice, once in its ascending part and once in its descending part at which point its slope changes. The only other points at which the slope changes are the boundaries of cell, meaning at the s_k's.

- Let $s \leq s_k$ such that $t^*(s) = t_k(s)$, then $K(s^+) = K(s^-) \uplus \{k\}$
- Let $s = s_k$, $\frac{\partial t^*}{\partial s}(s^+) = \frac{\partial t^*}{\partial s}(s^-) - \frac{2}{\sqrt{2}} \cdot \frac{w_k}{dw_0 + \sum_{k \in K(s)} w_k}$
- Let $s \geq s_k$ such that $t^*(s) = t_k(s)$, then $K(s^+) = K(s^-) \backslash \{k\}$

Moreover, because the (s_k, t_k) are Pareto points, t^* will meet the ascending part in ascending order, the s_k in ascending order and the descending part in ascending order.

Also, at $-\infty$, $t^*(s) = 0$ and it has null derivative. Using that and the rules above, we can track $t^*(s)$ in an efficient way. An example is provided in Figure 6. □

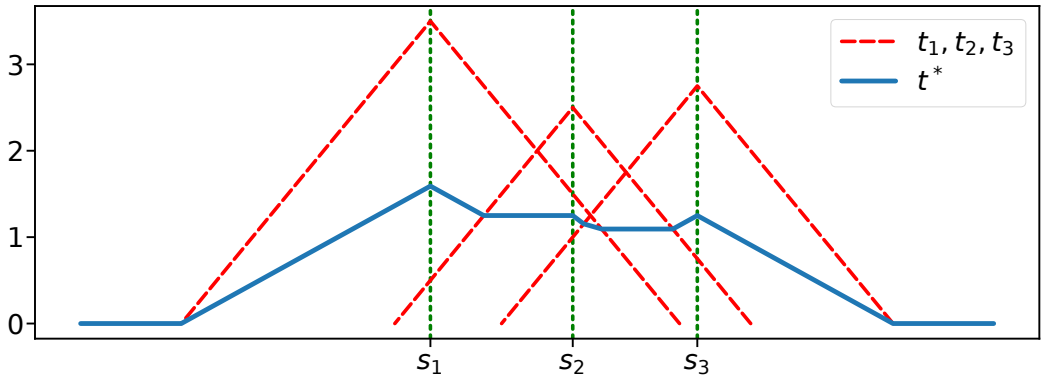

Figure 6: Example of t^* tracking

We can also compute the minimizer and the minimal value of $g_{k_0}(s, t^*(s))$ on a linear part of $t^*(s)$ by differentiating $g_{k_0,\varphi}(s,t)$ in s with $K(s)$ held constant. This gives rise to an algorithm which has complexity of order $p \log p$ where you need $p \log p$ operations to sort the Pareto front and then with complexity p you can range over the s-space keeping track of some sums and of t^* and computing the minimal value of $g_{k_0}(s, t^*(s))$ along with its minimizer. This reduces the run-time cost of the transport cost computation for adding a point from p^2 to $p \log p$ and for any point to $Kp + p \log p$ as the sorting cost can be dampened.

Moreover, while running Track-and-Stop, only a single point is ever updated between two subsequent minimal transportation cost computations meaning that the sort can be updated in linear time.

D.3 Experiments

We made some experiments to highlight the gain from using the improved algorithm for 2d rather than the generic one. For that, we picked p points forming a Pareto set in a 1010 square and we added a unique non Pareto optimal point at 0 in our point cloud. Then we measured the time used by each algorithm to compute the minimum transportation cost against a random vector of weights. We repeated the operation a thousand times for each tested p. We then reported t_2 the average time taken by the improved algorithm for an iteration, t_n the average time taken by the generic algorithm for an iteration and r the ratio between t_n and t_2. These experiments were done on a single core of an Intel(R) Core(TM) i5-6300U CPU.

Table 1: Comparison between the improved and generic algorithm

p	t_2 (s)	t_n (s)	r
2	7.33×10^{-4}	1.01×10^{-3}	1.38
4	1.05×10^{-3}	1.97×10^{-3}	1.88
8	1.69×10^{-3}	4.47×10^{-3}	2.65
16	3.00×10^{-3}	1.25×10^{-2}	4.17
32	5.68×10^{-3}	3.47×10^{-2}	6.11
64	1.02×10^{-2}	1.16×10^{-1}	11.4
128	2.25×10^{-2}	4.48×10^{-1}	19.9
256	4.91×10^{-2}	1.77	36.0
512	8.77×10^{-2}	7.66	87.3

E Experiments

In this Appendix, we give additional details about the experiments we ran. The first round of experiments was based on resampling real life data from the study [Munro et al., 2021]. We report in Table 2 and 3, the value from the study that we used to generate the data. Moreover the last column of Table 2 gives the optimal weight associated with each arm obtained by solving the optimization problem of Proposition 1. Lines written in a bold font correspond to the Pareto optimal arms and the underlined entry highlights a non-Pareto optimal arm that needs a lot of samples.

Table 2: Means and optimal weights of the different arms

Dose 1/Dose 2	Dose 3 (booster)	Anti-spike IgG	$NT._{50}$	cellular response	w^*
Prime BNT/BNT	ChAd	9.5	6.86	4.56	0.0077
	NVX	9.29	6.64	4.04	0.0016
	NVX Half	9.05	6.41	3.56	0.0007
	BNT	10.21	7.49	4.43	0.023
	BNT Half	10.05	7.2	4.36	0.0048
	VLA	8.34	5.67	3.51	0.00066
	VLA Half	8.22	5.46	3.64	0.00079
	Ad26	9.75	7.21	4.71	0.018
	m1273	**10.43**	**7.61**	**4.72**	**0.14**
	CVn	8.94	6.19	3.84	0.0011
Prime ChAd/ChAd	ChAd	7.81	5.26	3.97	0.0014
	NVX	8.85	6.59	4.73	0.021
	NVX Half	8.44	6.15	4.59	0.0089
	BNT	9.93	7.39	4.75	0.025
	BNT Half	8.71	7.2	4.91	<u>0.35</u>
	VLA	7.51	5.31	3.96	0.0014
	VLA Half	7.27	4.99	4.02	0.0015
	Ad26	8.62	6.33	4.66	0.013
	m1273	**10.35**	**7.77**	**5.0**	**0.38**
	CVn	8.29	5.92	3.87	0.0012

Table 3: Pooled variance for each immunogenicity trait

	Anti-spike IgG	$NT._{50}$	cellular response
Variance	0.70	0.83	1.54